*Progress In Electromagnetics Research*, PIER 89, 85–100, 2009

# SCATTERING BY A DIELECTRIC-LOADED CONDUCTING WEDGE WITH CONCAVED EDGE: TE CASE

**W.-G. Lim and J.-W. Yu**

Department of Electrical Engineering
Korea Advanced Institute of Science and Technology (KAIST)
Daejeon, 305-701, Korea

**Abstract**—The rigorous numerical formulation for TE-scattering from a conducting wedge with concaved edge is presented and numerical computations for scattered fields are shown. The radial mode matching technique is used to obtain the scattering field in a series form. The accuracy of the present method is checked with existing solutions of a semi-circular channel and sharp wedge, which are special case of the general geometry of a conducting wedge with concaved edge.

## 1. INTRODUCTION

The scattering by a H-polarized electromagnetic plane wave incident on a conducting wedge is well known and may be evaluated asymptotically as the sum of a geometrical optics term plus an edge-diffracted term as postulated by Keller [1]. Also, the effects of a physical edge (not perfectly sharp) have been extensively studied. Weiner and Borison [2] have divided an actual cone tip into ball-point tip, rounded tip and concaved tip to calculate RCS (radar cross section) of the cone tip. Similarly, physical wedge edge may be divided into cylinder-tip edge, rounded edge, and concaved edge. Scattering by a half plane with cylinder-tip edge has been investigated by Pozar [3] and many others, and scattering by a wedge with rounded edge has been studied by Ross and Hamid [4]. We investigated the behavior of a wedge with concaved edge for TM case [5].

The scattering by a semi-circular channel in a ground plane, which is the special case of the wedge with concaved edge, is of an interest to

Corresponding author: J.-W. Yu (drjwyu@ee.kaist.ac.kr).

many investigators [6–12]. This is due to the fact that this local guiding structure may excited internal resonances and it sometimes yield scattering contribution. The behavior of electromagnetic scattering from a semi-circularly-shaped crack in a conducting plane was first studied by Schdava for low-frequency scattering regime, was later studied numerically with the dual-eigenfunction series approach, and numerically with the Fourier-series expansion technique.

Most of previous work deals with scattering problem when the plane of incidence perpendicular to the wedge axis. Hence, the scattering behavior is not well understood when the plane of the incidence is at an arbitrary angle with respect to the wedge axis (three dimensional oblique incidence case). In this paper, a simple series solution for oblique scattering by a wedge with concaved edge or a semi-circular channel shown in Fig. 1 is investigated by using radial mode matching technique.

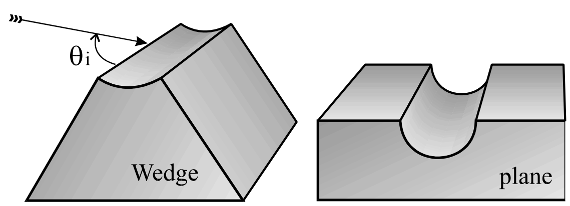


(a) (b)

**Figure 1.** (a) The perfectly conducting wedge with concaved edge, (b) a semi-circular channel.

## 2. FORMULATION OF MAGNETIC LINE-SOURCE SCATTERING

### 2.1. Field Representations

Assume that a magnetic line source is incident upon a wedge with concaved edge, as is shown in Fig. 2. Throughout the work, $e^{j\omega t}$ time harmonic factor is suppressed. In region (I) ($\rho > a$, $0 < \phi < \phi_o$) which satisfy the boundary condition $E_{tan} = 0$ on the wedge and the

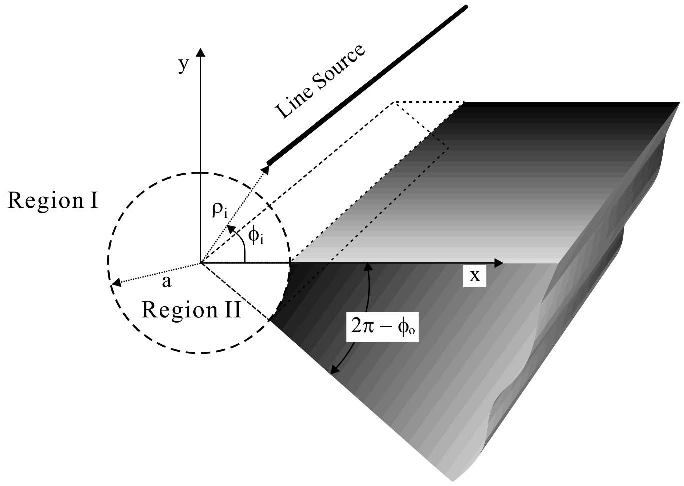


**Figure 2.** Magnetic line source scattering by a dielectric-loaded wedge with concaved edge.

radiation condition given by

$$H_z^I(\rho,\phi)=H_o^l\begin{cases}\displaystyle\sum_{p=0}^{\infty}\left\{s_p H_\mu^{(2)}(k_o\rho_i)J_\mu(k_o\rho)+B_p H_\mu^{(2)}(k_o\rho)\right\}\cos\mu\phi, & a<\rho<\rho_i\\ \displaystyle\sum_{p=0}^{\infty}\left\{s_p J_\mu(k_o\rho_i)H_\mu^{(2)}(k_o\rho)+B_p H_\mu^{(2)}(k_o\rho)\right\}\cos\mu\phi, & \rho>\rho_i\end{cases}\tag{1}$$

where

$$H_o^l = -\frac{k_o I_m}{4\eta_o}$$
$$s_p = \begin{cases}2\pi/\phi_o\cos\mu\phi_i, & p=0\\ 4\pi/\phi_o\cos\mu\phi_i, & p\neq 0\end{cases}$$
$$\mu = \frac{p\pi}{\phi_o}, p=0,1,2\ldots$$

In above expressions, $I_m$ is the strength of the magnetic current filament. Since $E_\phi = 1/(j\omega\varepsilon)\partial H_z(\rho,\phi)/\partial\rho$, the corresponding $\phi$

components of the E-field in region (I) are

$$E_\phi^I(\rho,\phi) = \frac{H_o^l k_o}{j\omega\varepsilon_o}\begin{cases}\sum_{p=0}^{\infty}\left\{s_p H_\mu^{(2)}(k_o\rho_i)J_\mu^{'}(k_o\rho)+B_p H_\mu^{(2)'}(k_o\rho)\right\}\cos\mu\phi, & a<\rho<\rho_i\\ \sum_{p=0}^{\infty}\left\{s_p J_\mu(k_o\rho_i)H_\mu^{(2)'}(k_o\rho)+B_p H_\mu^{(2)'}(k_o\rho)\right\}\cos\mu\phi, & \rho>\rho_i\end{cases} \tag{2}$$

In region (II) of wave number $k_1(=\omega\sqrt{\mu_o\epsilon_o\epsilon_r})$ ($\rho < a$, $0 < \phi < 2\pi$), the transmitted field inside the dielectric cylinder may be represented as

$$H_z^{II}(\rho,\phi) = H_o^l \sum_{n=-\infty}^{\infty} A_n J_n(k_1\rho)e^{jn\phi} \tag{3}$$

The corresponding electric field is

$$E_\phi^{II}(\rho,\phi) = \frac{H_o^l k_1}{j\omega\varepsilon_o\varepsilon_r}\sum_{n=-\infty}^{\infty} A_n J_n^{'}(k_1\rho)e^{jn\phi} \tag{4}$$

### 2.2. Matching Boundary Conditions ($\rho = a$)

To determine unknown coefficients $A_n$ and $B_p$, it is necessary to match the boundary conditions of tangential E- and H-field continuities at $\rho = a$.

First, the boundary condition at $\rho = a$ of the tangential H-field continuity across the aperture circular ($0 < \phi < \phi_o$) become

$$\sum_{p=0}^{\infty}\left\{s_p H_\mu^{(2)}(k_o\rho_i)J_\mu(k_oa)+B_p H_\mu^{(2)}(k_oa)\right\}\cos\mu\phi=\sum_{k=-\infty}^{\infty} A_k^{TE} J_k(k_1a)e^{jk\phi} \tag{5}$$

In above equation, applying orthogonality condition of cosine function with respect to $\phi$ from 0 to $\phi_o$, we obtain

$$s_q H_\nu^{(2)}(k_o\rho_i)J_\nu(k_oa) + B_q H_\nu^{(2)}(k_oa) = \frac{2}{\phi_o}\epsilon_q \sum_{k=-\infty}^{\infty} A_k J_k(k_1a)g_{k\nu} \tag{6}$$

where

$$g_{k\nu} = \int_0^{\phi_o} e^{jk\phi} \cos \nu\phi d\phi$$

$$\epsilon_q = \begin{cases} 0.5, & q = 0 \\ 1, & q \neq 0 \end{cases}$$

In a similar fashion, the boundary conditions at $\rho = a$ of zero tangential E-field on the crack ($\phi_o < \phi < 2\pi$) and continuous fields across the aperture circular ($0 < \phi < \phi_o$) become

$$\sum_{p=0}^{\infty} \left\{ s_p H_\mu^{(2)}(k_o\rho_i) J_\mu'(k_o a) + B_p H_\mu^{'(2)}(k_o a) \right\} \cos \mu\phi U_I = \frac{k_o}{k_1} \sum_{n=-\infty}^{\infty} A_n J_n'(k_1 a) e^{jn\phi} \quad (7)$$

where $U_I = 1$ for $0 < \phi < \phi_o$ and zero elsewhere. In above equation, applying orthogonality condition of exponential function with respect to $\phi$ from 0 to $2\pi$, we obtain

$$2\pi A_k J_k'(k_1 a) = \frac{k_1}{k_o} \sum_{p=0}^{\infty} \left\{ s_p H_\mu^{(2)}(k_o\rho_i) J_\mu'(k_o a) + B_p H_\mu^{'(2)}(k_o a) \right\} \hat{g}_{\mu k} \quad (8)$$

where

$$\hat{g}_{\mu k} = \int_0^{\phi_o} e^{-jk\phi} \cos \mu\phi d\phi$$

In order to determine the coefficient $B_p$, substituting (8) into (6), applying the Wronskian of the Bessel function, and rearranging this, we have

$$\sum_{p=0}^{\infty} \left\{ s_p H_\mu^{(2)}(k_o\rho_i) J_\mu(k_o a) + B_p H_\mu^{(2)}(k_o a) \right\} \left\{ \delta_{qp} - \frac{H_\mu^{(2)'}(k_o a)}{H_\mu^{(2)}(k_o a)} I_{qp} \right\} = \frac{2j}{\pi k_o a} \sum_{p=0}^{\infty} \frac{s_p H_\mu^{(2)}(k_o\rho_i)}{H_\mu^{(2)}(k_o a)} I_{qp} \quad (9)$$

where $\delta_{qp}$ is the Kronecker delta, and

$$I_{qp} = \frac{\epsilon_q}{\pi\phi_o} \frac{k_1}{k_o} \sum_{k=-\infty}^{\infty} \frac{J_k(k_1 a)}{J_k'(k_1 a)} g_{\nu k} \hat{g}_{\mu k}$$

Equation (9) can be solved numerically to obtain the constants $B_p$. The infinite series involved in the solution is convergent(which is illustrated in the Table 1), therefore it will be truncated after a certain number of terms which depend on the largest argument of the Bessel function (i.e., $ka$). Once $B_p$ is determined, it is possible to evaluate the coefficient $A_n$

**Table 1.** Convergence behavior of $B_p$ versus $p$ ($ka = 5, 10$, $\phi_i = \phi = 105°$ and $\phi_o = 210°$) ($B_1 = B_3 = B_5 = B_7 = \cdots = 0.0$).

| | $B_p$ | |
|---|---|---|
| $p$ | $ka = 5$ | $ka = 10$ |
| 0 | $-1.8593 - j1.6314$ | $-0.0050 + j0.4414$ |
| 2 | $-2.5460 + j1.5338$ | $-0.2484 + j1.7388$ |
| 4 | $-0.5822 + j2.2346$ | $-0.2034 - j0.1842$ |
| 6 | $-0.0288 + j0.8006$ | $+1.5196 + j1.5915$ |
| 8 | $+0.0104 + j0.1503$ | $+2.4664 + j2.7850$ |
| 10 | $+0.0025 + j0.0191$ | $+1.6500 + j1.8575$ |
| 12 | $+0.0003 + j0.0017$ | $+0.6631 + j0.7333$ |
| 14 | | $+0.1846 + j0.1999$ |
| 16 | | $+0.0384 + j0.0407$ |
| 18 | | $+0.0062 + j0.0065$ |

## 2.3. Scattered Field Computation

### *2.3.1. Plane Wave Scattering*

The analysis has been done for the line source excitation. Plane wave excitation is obtained by letting the line source recede to infinity. When the source is placed at far distances ($k_o\rho \gg 1$ and $\rho_i > \rho$) and the observations are made at any point, then total magnetic field of Equation (1) can be written, by replacing the Hankel function $H_\mu^{(2)}(k\rho_i)$ by its asymptotic form, as

$$H_z^I(\rho,\phi) \overset{k_o\rho_i \to \infty}{\simeq} H_o^l \sqrt{\frac{2j}{\pi k_o}} \frac{e^{-jk_o\rho_i}}{\sqrt{\rho_i}} \sum_{p=0}^{\infty} \left\{ s_p j^\mu J_\mu(k_o\rho) + B_p H_\mu^{(2)}(k_o\rho) \right\} \cos\mu\phi \tag{10}$$

*2.3.2. Far-Zone Field*

When the observations are made in the far zone ($k_o\rho \gg 1,\ \rho > \rho_i$), the scattered field by plane wave and line source can be written, by replacing the Hankel function $H_\mu^{(2)}(k_o\rho)$ by its asymptotic expression, as

$$H_z^{far} = H_o^l\sqrt{\frac{2}{\pi k_o\rho}}e^{-j(k_o\rho-\pi/4)}P_h(\phi) \tag{11}$$

where

$$P_h(\phi) = \sum_{p=0}^{\infty} j^\mu B_p \cos\mu\phi \tag{12}$$

The scattering properties of two-dimensional bodies of infinite length are conveniently described in terms of the echo width, i.e.

$$W(\phi) = \frac{4}{k_o}|P_h(\phi)|^2 \tag{13}$$

*2.3.3. Diffraction Coefficient*

To obtain the total magnetic field of a $TE_z$ plane wave incident in the far zone, the asymptotic expansion of the Hankel function for a large argument is employed together with the well-known approximation for the field diffracted by a sharp wedge. The total scattered field may be expressed as

$$\frac{H_z^s}{H_z^i} \sim \frac{e^{-j(k\rho+\pi/4)}}{\sqrt{2\pi k\rho}}\left\{\frac{\sin(\pi/n)}{n}\left[\frac{1}{\cos\left(\pi/n\right)-\cos\left((\phi-\phi_i)/n\right)}\right.\right.$$
$$\left.\left.+\frac{1}{\cos\left(\pi/n\right)-\cos\left((\phi+\phi_i)/n\right)}\right]+2j\sum_{p=0}^{\infty} j^\mu B_p\cos\mu\phi\right\} \tag{14}$$

where $n = \phi_o/\pi$.

In Equation (14), the first term is the field by a sharp wedge ($H_z^w/H_z^i$) and the second term represents a perturbation term ($H_z^p/H_z^i$) for concaved edge. Furthermore, if $ka$ is not too large compared to unity, the geometrical optics component of perturbation term can be neglected and the concaved edge may also regarded as simply modifying the diffraction properties of the edge. Under this condition, the field of perturbation term may be expressed as the product of the incident field times diffraction coefficient $D_h$ by concaved edge, i.e.,

$$H_z^p = H_z^i D_h(ka, \phi_o, \phi, \phi_i) \frac{e^{-jk\rho}}{\sqrt{\rho}} \tag{15}$$

where

$$D_h(ka, \phi_o, \phi, \phi_i) = \sqrt{\frac{2}{\pi k}} e^{j\pi/4} \sum_{p=0}^{\infty} j^{\mu} B_p^{TE} \cos \mu\phi \tag{16}$$

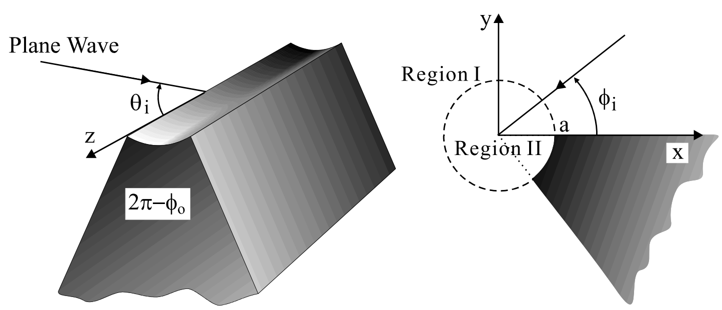


**Figure 3.** Oblique incidence plane wave scattering of a conducting wedge with concaved edge.

## 3. FORMULATION OF OBLIQUE INCIDENCE PLANE WAVE SCATTERING

### 3.1. Field Representations

Consider a $TE_z$ plane wave at $\phi = \phi_i$ and $\theta = \theta_i$ illuminating an infinite, perfectly conducting wedge with concaved edge as shown in Fig. 3. The expression for the total magnetic field in region I $(\rho > a, 0 < \phi < \phi_o)$ which satisfy the boundary condition $E_{tan} = 0$ on the wedge and the radiation condition is given by

$$H_z^I(\rho, \phi) = F(\theta_i) \sum_{p=0}^{\infty} \{s_p j^{\mu} J_{\mu}(\kappa\rho) + B_p H_{\mu}^{(2)}(\kappa\rho)\} \cos \mu\phi \tag{17}$$

where

$$\begin{aligned} s_p &= \frac{4\varepsilon_p \pi}{\phi_o} \cos \mu\phi_i, \mu = \frac{p\pi}{\phi_o} \\ F(\theta_i) &= \sin \theta_i e^{jkz \cos \theta_i} \\ \kappa &= k \sin \theta_i \end{aligned}$$

and $k$ is a wave number of free space$(= w\sqrt{\mu_o\epsilon_o})$ and $\varepsilon_p = 0.5$ for $p = 0$ and 1 for $p \neq 0$. $J_\mu$ and $H_\mu^{(2)}$ are Bessel function of $\mu$th order and the first kind and Hankel function of $\mu$th order and the second kind, respectively. In region II ($\rho < a$) of wave number $k$, the total magnetic field may be represented as a summation of radial waveguide modes, i.e.,

$$H_z^{II}(\rho,\phi) = F(\theta_i)\sum_{n=-\infty}^{\infty} A_n J_n(\kappa\rho)e^{jn\phi} \tag{18}$$

Since $E_\phi(\rho,\phi) = 1/(jw\epsilon_o)\partial H_z(\rho,\phi)/\partial\rho$, the corresponding $\phi$ components of the E-field are

$$E_\phi^I(\rho,\phi) = \frac{\kappa F(\theta_i)}{jw\epsilon_o}\sum_{p=0}^{\infty}\{s_p j^\mu J_\mu'(\kappa\rho) + B_p H_\mu^{(2)'}(\kappa\rho)\}\cos\mu\phi \tag{19}$$

$$E_\phi^{II}(\rho,\phi) = \frac{\kappa F(\theta_i)}{jw\epsilon_o}\sum_{n=-\infty}^{\infty} A_n J_n'(\kappa\rho)e^{jn\phi} \tag{20}$$

To determine the unknown coefficients $A_n$ and $B_p$, it is necessary to match the boundary conditions of tangential E- and H-field continuities at $\rho = a$. The boundary conditions of the zero tangential electric field at $\rho = a$ and on the conductor and continuous fields (i.e., $H_z$ and $E_\phi$) across the aperture are applied to obtain

$$\sum_{p=0}^{\infty}\{s_p j^\mu J_\mu(\kappa a)+B_p H_\mu^{(2)}(\kappa a)\}\left\{\delta_{qp}-\frac{H_\mu^{(2)'}(\kappa a)}{H_\mu^{(2)}(\kappa a)}\right\}I_{qp}=\frac{2j}{\pi\kappa a}\sum_{p=0}^{\infty}\frac{s_p j^\mu}{H_\mu^{(2)}(\kappa a)}I_{qp} \tag{21}$$

$$A_n J_n'(\kappa a) = \frac{1}{2\pi}\sum_{p=0}^{\infty}\{s_p j^\mu J_\mu'(\kappa a) + B_p H_\mu^{(2)'}(\kappa a)\}\hat{g}_{\mu n} \tag{22}$$

where $\delta_{qp}$ is the Kronecker delta and

$$\begin{aligned} I_{qp} &= \frac{\varepsilon_q}{\pi\phi_o}\sum_{n=-\infty}^{\infty}\frac{J_n(\kappa a)}{J_n'(\kappa a)}g_{\nu n}\hat{g}_{\mu n} \\ g_{\nu n} &= \int_0^{\phi_o} e^{jn\phi}\cos\nu\phi d\phi \\ \hat{g}_{\mu n} &= \int_0^{\phi_o} e^{-jn\phi}\cos\mu\phi d\phi \end{aligned}$$

where $\nu = q\pi/\phi_o, q = 0, 1, 2, \cdots$, and $\varepsilon_q = 0.5$ for $q = 0$ and 1 for $q \neq 0$.

Equation (21) can be solved numerically to obtain the coefficients $B_p$. The infinite series involved in the solution are highly convergent, therefore it will be truncated after a certain number of terms.

## 3.2. Scattered Field Computation

### *3.2.1. Diffraction Coefficient*

To obtain the scattered field for $TE_z$ plane wave, asymptotic expansion of the Hankel function for a large argument is employed together with the well-known approximation for the field diffracted by a sharp wedge. The total scattered field may be expressed as

$$\frac{H_z^s}{H_z^i} \sim \frac{e^{-j(k\rho+\pi/4)}}{\sqrt{2\pi k\rho}\sin\theta_i}\left\{\frac{\sin(\pi/n)}{n}\left[\frac{1}{\cos(\pi/n) - \cos((\phi-\phi_i)/n)}\right.\right.$$
$$\left.\left. + \frac{1}{\cos(\pi/n) - \cos((\phi+\phi_i)/n)}\right] + 2j\sum_{p=0}^{\infty} j^\mu B_p \cos\mu\phi\right\} \quad (23)$$

where $n = \phi_o/\pi$.

In Equation (23), the first term is the field by a sharp wedge $(H_z^w/H_z^i)$ and the second term represents a perturbation term $(H_z^p/H_z^i)$ for the concaved edge. Furthermore, if $\kappa a$ is not too large compare to unity, the geometrical optics component of perturbation term may be expressed as the product of the incident field times diffraction coefficient $D_h$, i.e.,

$$H_z^p = H_z^i D_h(\kappa a, \phi_o, \phi, \phi_i, \theta_i)\frac{e^{-jk\rho}}{\sqrt{\rho}} \quad (24)$$

where

$$D_h(\kappa a, \phi_o, \phi, \phi_i, \theta_i) = \sqrt{\frac{2}{\pi k}}\frac{e^{j\pi/4}}{\sin\theta_i}\sum_{p=0}^{\infty} j^\mu B_p \cos\mu\phi \quad (25)$$

and $D_h$ is a diffraction coefficient of the concaved edge in the case of oblique incidence.

## 4. NUMERICAL RESULTS

To check the accuracy of our calculations, the special case of a semi-circular channel in a ground plane is introduced. In this case the aperture angle $\phi_o$ in our geometry is set to $\pi$. The magnitude of the normalized backscattered field pattern $|P_h|$ is calculated and plotted versus $ka$ at different values of $\phi_o$ as shown in Fig. 4. Comparison between our results and their correspondence in [10] showed an excellent agreement.

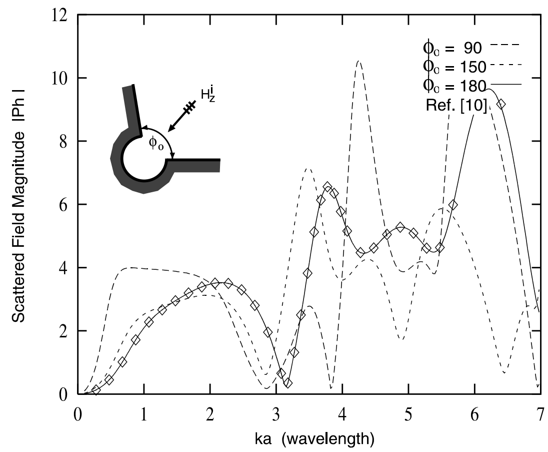


**Figure 4.** The backscattered field magnitude $|P_h(\phi)|$ versus $ka$ for three different aperture angles ($\phi_o = 90°, 150°, 180°$) and $\phi_i = \phi = \phi_o/2$.

Figure 5 shows the behavior of the normalized backscattered field magnitude $|P_h|$ versus $ka$ for the three different aperture angles ($\phi_o = 90°, 150°, 180°$) at normal incidence($\phi_i = \phi_o/2$) when $\varepsilon_r = 3.0$. In view of Figs. 4 and 5, it is also seen that a presence of the dielectric loading tends to decrease a period of the resonance versus $ka$, and also seen that narrowing the angle of aperture enhances the resonant scattering pattern.

Figure 6 shows the behavior of the backscattered field magnitude $|P_h|$ versus $ka$ for the semi-circular crack at three different oblique incidence. Three curves are shown corresponding to normal incidence ($\phi_i = 90°, \theta_i = 90°$) and oblique incidences ($\phi_i = 90°, \theta_i = 60°$ and $\phi_i = 60°, \theta_i = 60°$).

Figure 7 shows normalized backscattered field of $H_z^s/H_z^i$ versus $\phi$ as a function of $ka$ for a $90°$ wedge. It is note that the numerical data for $ka = 0$ case agrees well with $90°$ sharp wedge backscattered field pattern. An increase in $ka$ causes an increase in the pattern. Phase data presented in radians are continuous except for a of $\pi$ radians at $\phi = \pi/2$ and $\pi$, which originates in the singular behavior of the asymptotic results for the sharp wedge.

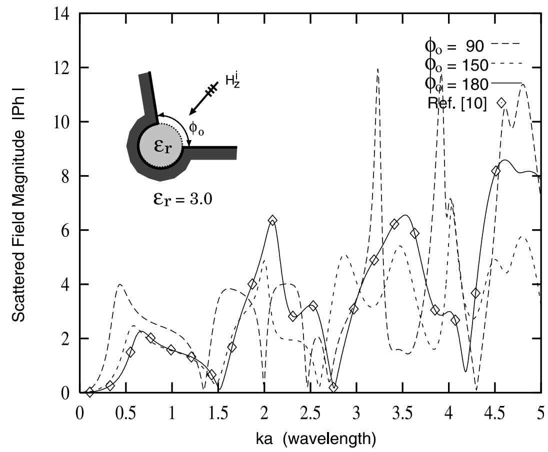


**Figure 5.** Normalized backscattered field of $H_z^s/H_z^i$ versus $\phi$ as a function of $ka$ for a 90° wedge.

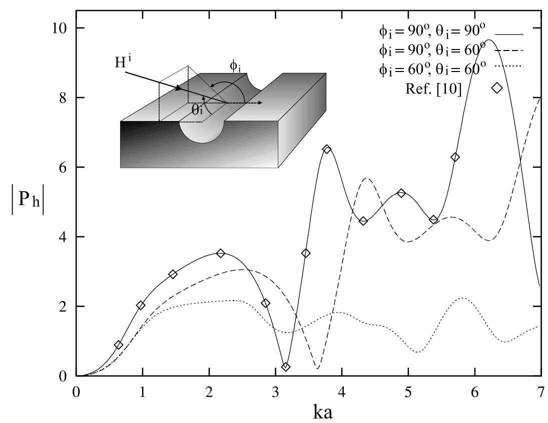


**Figure 6.** The backscattered field magnitude $|P_h|$ versus $ka$ for the semi-circular crack at three different oblique incidence.

Figure 8 shows normalized backscattered field of $H_p^s/H_z^i$ versus $\phi$ as a function of $ka$ of a 90° wedge. Fig. 9 shows normalized backscattered field of $H_z^s/H_z^i$ versus $\phi$ as a function of $\epsilon_r$ for a dielectric cylinder loaded wedge with concaved edge of $ka = 0.5$ and $\phi_o = 270°$. It is show that the cylindrical dielectric cylinder cap leads to significant variations in the diffraction pattern of the wedge. Fig. 10 shows a normalized field pattern for the wedge with concaved edge of $\phi_o = 270°, \phi_i = 225°$ and $2a = 1\lambda$ in the case of three different oblique

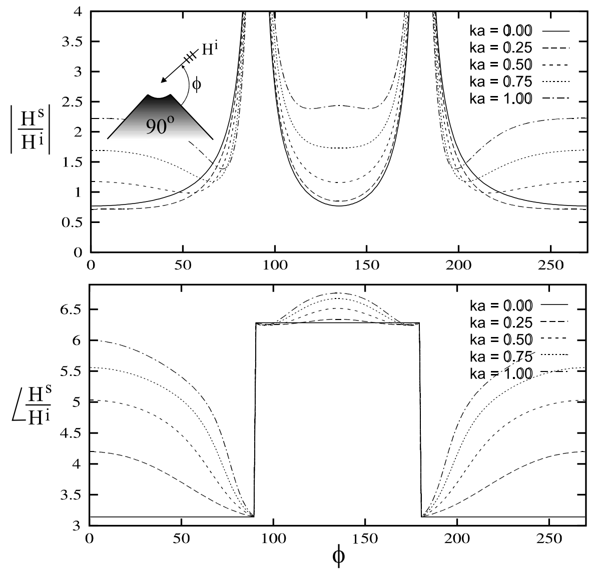


**Figure 7.** Normalized backscattered field of $H_z^s/H_z^i$ versus $\phi$ as a function of $ka$ for a 90° wedge.

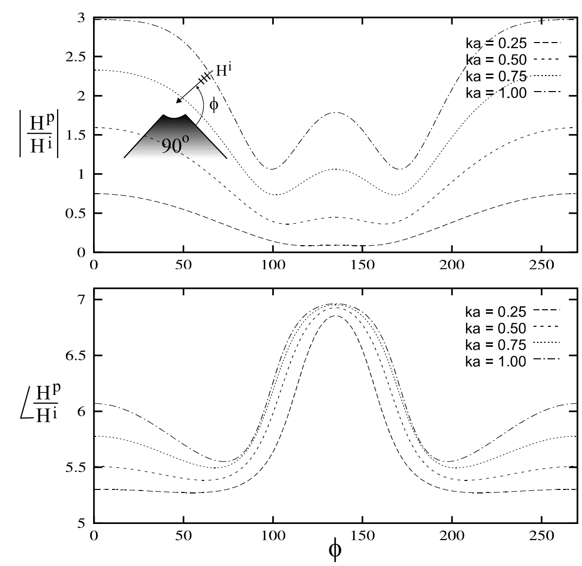


**Figure 8.** Normalized backscattered field of $H_z^p/H_z^i$ versus $\phi$ as a function of $ka$ for a 90° wedge.

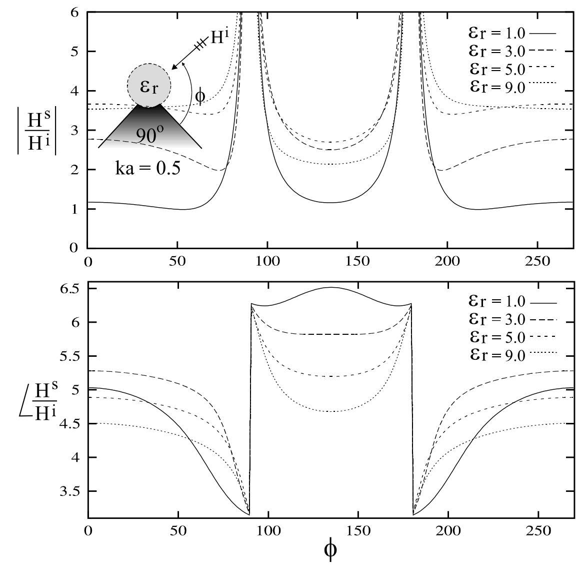


**Figure 9.** Normalized backscattered field of $H_z^s/H_z^i$ versus $\phi$ as a function of $\epsilon_r$ for a $90°$ wedge with dielectric cylinder of $ka = 0.5$.

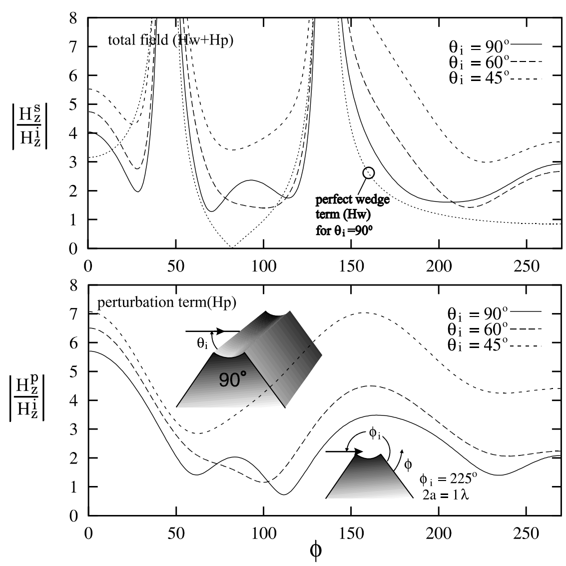


**Figure 10.** Normalized field pattern for the wedge with concaved edge of $\phi_o = 270°, \phi_i = 225°$, and $\phi_i = 225°$ and $2a = 1\lambda$ in the case of four different oblique incidence of $\theta_i = 30°, 45°, 60°$ and $90°$.

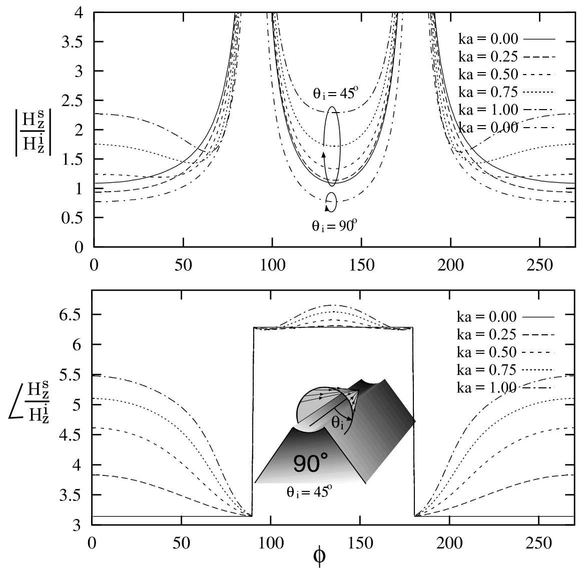


**Figure 11.** Normalized backscattered field of $H_z^s/H_z^i$ versus $\phi$ for different $ka$ of a 90° wedge in the case of oblique incidence ($\theta_i = 45°$).

incidence of $\theta_i = 45°, 60°$ and 90°. As $\theta_i$ decrease, the level of the total field pattern increase as shown in figure. Normalized backscattered field of $H_z^s/H_z^i$ versus $\phi$ is shown in Fig. 11 for different $ka$ of a 90° wedge in the case of oblique incidence ($\theta_i = 45°$).

## 5. CONCLUSIONS

The mathematical formulation for TE-scattering from a wedge with concaved edge is presented and numerical computations for scattered fields are shown. The formulation is simple to used so that it may not only help us understand the oblique scattering behaviors from a wedge with concaved edge and a semi-circular channel, but also provide a means to crosscheck with other arbitrarily-shaped wedge and channel scattering results.

## REFERENCES

1. Keller, J. B., "Diffraction by an aperture," *J. Appl. Phys.*, Vol. 28, 426–444, Apr. 1957.
2. Weiner, S. D. and S. L. Borison, "Radar scattering from blunted

cone tips," *IEEE Trans. Antennas Propagat.*, Vol. 14, 774–781, Nov. 1966.

3. Pozar, D. M. and E. H. Newman, "Near field of a vector electric line source near the edge of a wedge," *Radio Science*, Vol. 14, 397–403, May–June 1979.
4. Ross, R. A. and M. A. K. Hamid, "Scattering by a wedge with rounded edge," *IEEE Trans. Antenna Propagat.*, Vol. 19, No. 4, 507–516, July 1971.
5. Yu, J.-W. and N.-H. Myung, "TM scattering by a wedge with concaved edge," *IEEE Trans. Antennas Propagat.*, Vol. 45, 1315–1316, Aug. 1997.
6. Scchdeva, B. K. and R. A. Hurd, "Scattering by a dielectric loaded trough in a conducting plane," *J. of Appl. Phys.*, Vol. 48, No. 4, 1473–1476, Apr. 1977.
7. Hinders, M. K. and A. D. Yaghjian, "Dual series solution to scattering from a semicircular channel in a ground plane," *IEEE Microwave and Guided Wave Letters*, Vol. 1, No. 9, 239–242, Sept. 1991.
8. Ragheb, H. A., "Electromagnetic scattering from a coaxial dielectric circular cylinder loading a semicircular gap in a ground plane," *IEEE Microwave Theory and Tech.*, Vol. 43, No. 6, 1303–1309, June 1995.
9. Park, T. J., H. J. Eom, W.-M. Boerner, and Y. Yamaguchi, "TM-scattering from a dielectric-loaded semi-circular trough in a conducting plane," *IEICE Trans. Commun.*, Vol. E75-B, No. 2, 87–91, Feb. 1992.
10. Park, T. J., H. J. Eom, Y. Yamaguchi, W.-M. Boerner, and S. Kozaki, "TE-plane wave scattering from a dielectric-loaded semi-circular trough in a conducting plane," *Journal of Electromagnetic Waves and Applications*, Vol. 7, No. 2, 235–245, Feb. 1993.
11. Yu, J.-W. and N.-H. Myung, "TM scattering by a coaxial dielectric-loaded circularly-shaped crack in a conducting wedge," *Asia-Pacific Microwave Conference*, New-Delhi, India, Dec. 1996.
12. Shen, T., W. Dou, and Z. Sun, "Gaussian beam scattering from a semicircular channel in a conducting plane," *Progress In Electromagnetics Research*, PIER 16, 67–85, 1997.